GEOPHYSICS, VOL. 84, NO. 3 (MAY-JUNE 2019); P. O63–O72, 6 FIGS., 2 TABLES.
10.1190/GEO2018-0007.1

Seismic attribute benchmarking on instantaneous frequency

Liyuan Xing[1], Victor Aarre[2], Arthur E. Barnes[3], Theoharis Theoharis[1], Nader Salman[2], and Egil Tjåland[4]

ABSTRACT

The complex seismic trace analysis is a widely applied and versatile method for computing seismic attributes. Instantaneous frequency is an important complex trace attribute, and it is generally used for identifying specific seismic events, such as abnormal attenuation and thin bed tuning. Although the definition itself is clear, in practice, the calculation varies considerably and deviates from the definition. As a result, there is little consistency in the calculation of the instantaneous frequency. We thus adopt a robust and reliable scientific process to objectively compare various implementations of the instantaneous frequency. To this end, we start by reviewing four classic algorithms for instantaneous frequency computation and efficient approximations and point out several issues and weaknesses of these algorithms. Then, the theoretical foundation for the instantaneous frequency of the sum of two sinusoids is derived from the original definition. With the above foundations, two synthetic test data sets of seismic traces, with varying frequencies and fixed amplitudes, are generated. Their synthetic ground truth instantaneous frequencies are automatically calculated by an analytic formula. In addition, regions that exhibit algorithmically interesting issues are segmented from the whole data sets and considered specifically in the proposed quality metrics. The evaluation includes four classic noncommercial algorithms and four commercial software implementations. Their quantitative and qualitative results indicate the effectiveness of the synthesized data sets and the quality metrics for instantaneous frequency evaluations. It is hoped that the inclusion of instantaneous frequency in the free academic benchmarking web service A3Mark will help to improve instantaneous frequency algorithms throughout the industry.

INTRODUCTION AND BACKGROUND

Seismic attributes measure characteristics or properties of seismic reflection data. They are analyzed to enhance information that might be hidden or be too subtle in a traditional seismic image, leading to a better geologic or geophysical interpretation of the data. Examples of seismic attributes include measured time, amplitude, frequency, and attenuation (SEG wiki, 2019).

In the highly competitive world of commercial seismic interpretation software, many seismic attributes implement intrinsically the same functionality, while having very different results even when fed with exactly the same input data (Barnes, 2006). In our previous work (Xing et al., 2018), we have built the first publicly available, independent (academic), free of charge, online web service (A3Mark) to objectively and reliably compare functionally similar structural seismic attributes, including discontinuity, dip angle, dip azimuth, and curvature. In this study, we expand our offering beyond the confines of geometric attributes in the time domain, and we attack the challenging measurement of frequency, which is regarded as one of the physical attributes (Taner et al., 1994).

Frequency attributes separate and classify seismic events within each trace based on their frequency content. They are useful in stratigraphic interpretation, such as in identifying abnormal attenuation and thin bed tuning. The first complex seismic trace attributes (introduced in 1977) included a frequency attribute, instantaneous frequency, as well as amplitude envelope, instantaneous phase, and apparent polarity (Chopra and Marfurt, 2005; SEG Wiki, 2019).

Manuscript received by the Editor 9 January 2018; revised manuscript received 20 November 2018; published ahead of production 01 February 2019; published online 29 March 2019.
[1]Norwegian University of Science and Technology, Department of Computer Science, Trondheim, Norway. E-mail: liyuan.xing@ntnu.no; theotheo@idi.ntnu.no.
[2]Schlumberger Information Solutions, Schlumberger AS, Stavanger, Norway. E-mail: vaarre@slb.com; nsalman@slb.com.
[3]Pagosa Geophysical Research, Pagosa Springs, Colorado, USA. E-mail: abarnes@pagosageophysical.com.
[4]Norwegian University of Science and Technology, Department of Geoscience and Petroleum, Trondheim, Norway. E-mail: egil.tjaland@ntnu.no.

Despite the wide use of instantaneous frequency, its computation varies widely. There exist a variety of ways, simple and elaborate, to get the instantaneous frequency calculation wrong, as reviewed in the next section. Different (or even the same) software platforms provide different calculations for instantaneous frequency.

Our goal is to propose a robust and reliable scientific process to compare various instantaneous frequency algorithms. To this end, we generate two synthetic test data sets of seismic traces with a wide range of frequencies, for which we also analytically derive the corresponding "synthetic ground truth" values for the instantaneous frequency. We propose several quality metrics in different instantaneous frequency regions, covering different aspects of the weakness of instantaneous frequency algorithms. Finally, preliminary tests are done by quantifying the difference between the algorithm results and the analytical synthetic ground truth. Quantitative and qualitative benchmarking results are given, e.g., quality metrics and error plots.

The remainder of this paper is organized as follows. In the next section, we give a definition of instantaneous frequency, review some classic algorithms for its computation and efficient approximations, and summarize their issues and weaknesses. Then, in the "Instantaneous frequency algorithm evaluation methodology" section, we first generate two complicated synthetic data sets of seismic traces from the sum of two sinusoids with varying frequencies and fixed amplitudes for test purposes, their synthetic ground truth of instantaneous frequency is calculated by deriving the theoretical foundation for the instantaneous frequency of two composited sinusoids from the original definition, and then we propose some quality metrics in different instantaneous frequency regions to reflect and measure the algorithm's performance. Finally, the "Results and discussion" section reports the evaluation results quantitatively and qualitatively, followed by some observations.

INSTANTANEOUS FREQUENCY

We start with a definition of instantaneous frequency and give typical computations and efficient approximations as well as related issues.

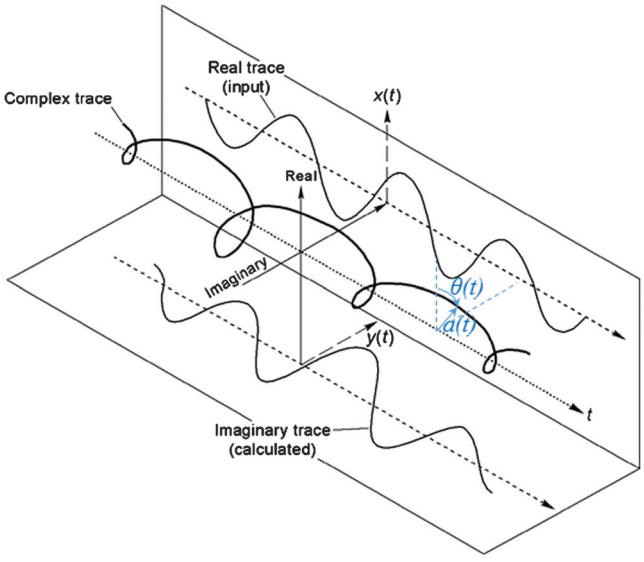

Figure 1. A complex seismic trace and its instantaneous attributes, from PetroWiki (2019).

Complex trace analysis and instantaneous frequency definition

Complex seismic trace analysis treats the seismic trace as if it was a continuous succession of sinusoids that all have constant frequency and amplitude. As shown in Figure 1, the recorded seismic trace $x(t)$ is the real part of the complex trace. Phase shifting the recorded trace by 90° through the Hilbert transform operator $h(t)$ yields the quadrature trace or the Hilbert-transformed trace, $y(t) = h(t) * x(t)$, which forms the imaginary part of the complex trace. Thus, the complex seismic trace is $z(t) = x(t) + iy(t)$.

From the complex trace $z(t)$, seismic attributes such as the instantaneous amplitude $a(t) = sqrt(x^2(t) + y^2(t))$, instantaneous phase $\theta(t) = \arctan(y(t)/x(t))$, and instantaneous frequency $f(t) = \frac{1}{2\pi}\frac{d\theta(t)}{dt}$ are derived. The instantaneous frequency is the time derivative of the instantaneous phase scaled to units of hertz. At a given time, for a relatively constant envelope, the instantaneous frequency represents the frequency of the sinusoid that matches the seismic trace in a small window about that time (Scheuer and Oldenburg, 1988). More details regarding their definitions and explanations can be found in Taner et al. (1979).

Turning this around, the seismic and quadrature traces can be expressed in terms of the instantaneous amplitude and instantaneous phase as $x(t) = a(t)\cos(\theta(t))$ and $y(t) = a(t)\sin(\theta(t))$, respectively. This is the essence of complex seismic trace analysis — separating the amplitude information from the phase information in seismic data (Taner and Sheriff, 1977; Taner et al., 1979).

Classic instantaneous frequency algorithms

The aforementioned definition of instantaneous frequency is unsuitable for the practical computation of instantaneous frequency because instantaneous phase is discontinuous and cannot be continuously differentiated. To get around this issue, the "exact formula" for instantaneous frequency, given by Taner et al. (1979), is

$$f(t) = \frac{1}{2\pi}\frac{x(t)y\prime(t) - x\prime(t)y(t)}{x^2(t) + y^2(t)}. \quad (1)$$

This formula can be implemented either in the time domain or in the frequency domain. This formula requires two derivatives. Most commercial code implements approximations for instantaneous frequency in the time domain. Coders seem not to like the derivative filter, so they use various difference equations instead, even though they generally use a standard Hilbert transform operator in the time domain. Claerbout's (1985, p. 20; see also Yilmaz, 2001, p. 1907) approximation is widely used:

$$f(t) \approx \frac{2}{\pi T}\frac{x(t)y(t+T) - x(t+T)y(t)}{(x(t) + x(t+T))^2 + (y(t) + y(t+T))^2}, \quad (2)$$

where T is the sample period. This equation involves two approximations in its derivation. It introduces a half-sample period time shift, and its results can exceed the Nyquist frequency. It gives poorer results at higher frequencies, and it becomes unreliable above about the half Nyquist. Scheuer and Oldenburg (1988) provide an alternative approximation:

$$f(t) \approx \frac{1}{2\pi T}\arctan\frac{x(t)y(t+T) - x(t+T)y(t)}{x(t)x(t+T) + y(t)y(t+T)}. \quad (3)$$

This approximation is more accurate at high frequencies than Claerbout's (1985) approximation above. Its values do not exceed Nyquist frequency, so in practice, it seems easier to work with than with the exact formula of equation 1, whose values are theoretically unbounded. Both approximations imply a half-sample shift downward in time. We remove this shift by averaging adjacent samples, which slightly smooths the results.

The frequency domain computation described in Hardage (1987, p. 220) basically uses the same time domain equation 1, but it has the Hilbert transform and the derivative operations performed in the frequency domain with fast Fourier transform. Specifically, it involves one forward transform and two inverse transforms, one to give $y(t)$ and the other to give the derivatives $x'(t)$ and $y\prime(t)$, as follows:

$$Y(f) = H(f)X(f), \tag{4}$$

$$y(t) \overset{F}{\Leftrightarrow} Y(f), \tag{5}$$

$$y\prime(t) \overset{F}{\Leftrightarrow} i2\pi f Y(f) \quad \text{and} \quad x\prime(t) \overset{F}{\Leftrightarrow} i2\pi f X(f), \tag{6}$$

where $H(f)$ and $X(f)$ are the Fourier transforms of the Hilbert transform operator $h(t)$ and seismic trace $x(t)$, respectively, and thus, $Y(f)$ is the Fourier transform of the quadrature trace $y(t)$. This avoids the need for long convolutional operators for the Hilbert transform and the derivative, which needs to be applied twice to produce $x'(t)$ and $y\prime(t)$; therefore, it is much faster. In principle, it is more accurate, but it can fail badly on unusual data that suffer severe wraparound effects, such as data with strong amplitudes at early times and weak amplitudes at late times.

Based on these published approaches (exact formula by Taner et al. [1979], frequency domain approach by Hardage [1987], Claerbout [1985] approximation, and Scheuer and Oldenburg [1988] approximation), several variants such as making "corrections" by changing the sign of all negative frequencies or bounding within the Nyquist frequency, have been used. It seems that everybody has a different way to compute this attribute. There are also many newer methods purporting to provide robust instantaneous frequency measures, but their robustness comes either from the fact that they are not truly instantaneous, or because they change the concept of instantaneous frequency (Hardy et al., 2003; Battista et al., 2007; Lu and Zhang, 2011; Wang and Gao, 2012).

Common issues with instantaneous frequency algorithms

The issues of the instantaneous frequency computations that we review are summarized as follows.

Differentiation operator issue

Software developers use the Hilbert transform operator but often avoid the derivative operator, even though it is similar. Instead, they use various difference equations (Claerbout, 1985; Scheuer and Oldenburg, 1988; Yilmaz, 2001); see equations 2 and 3 above. A standard two-point difference operator performs satisfactorily in place of a derivative filter, but it implies a half-sample time shift in the output, which is undesirable. One solution is to use a three-point difference operator centered on the current sample, which creates no shift. This works fine up to the half Nyquist, but it aliases above that frequency. This issue can be solved by resampling the data to half the sample period prior to the differencing, but it requires a long sinc interpolator, which may introduce its own amplitude errors at higher frequencies and increases the computation time. Another solution is to use the frequency domain equation 6, or to apply adjacent sample averaging and tolerate the slight smearing that this causes.

Low-frequency issue

Low frequencies down to approximately 3 Hz exist in modern "broadband" seismic data and must be supported. To preserve these low frequencies in the Hilbert transformation, the operator length must be sufficiently long. In the time domain, this is achieved by using a very long Hilbert transform operator. Alternatively, it is implicitly solved using the frequency-domain Hilbert transform, equation 4. A frequency-domain approach is much faster and can be used for the Hilbert transformation and for differentiation.

Frequency spike issue

Large frequency spikes beyond the Nyquist frequency are, in some sense, the least important part of an instantaneous frequency trace because they occur at amplitude minima, where the seismic signal is weakest. In theory, a frequency spike can reach infinite magnitude, which occurs when the denominators in the equations for instantaneous frequency (equations 1 and 12) are zero. Some methods, such as Scheuer and Oldenburg's (1988) approximation, limit the spike magnitude to the Nyquist frequency.

Negative frequency issue

The issue of frequency spikes and negative frequencies tends to discomfit geophysicists, though they are comfortable with negative Fourier spectral frequencies. As a result, one often reads that instantaneous frequency produces "nonphysical values." This is incorrect. Fourier spectral frequency and instantaneous frequency are two different but equally valid ways of looking at the same problem. Interestingly, they both yield exactly the same answers when averaged appropriately (Ville, 1948; Cohen, 1995, p. 9).

Filter tail issue

This is a problem common to any filtering process because of the filter operator length. In instantaneous frequency calculations, filter tails result from the Hilbert transform and the derivative convolutional operators. If a frequency-domain approach is used, then the filter tail problem sometimes also includes noticeable wraparound effects that can be mitigated by padding the data with zeros.

INSTANTANEOUS FREQUENCY ALGORITHM EVALUATION METHODOLOGY

The benchmarking of instantaneous frequency algorithms requires suitable test data sets and evaluation metrics. We design two data sets of seismic traces, as well as their synthetic ground truth instantaneous frequencies, and we propose region-based quality metrics to reflect the various issues of the algorithms quantitatively.

Generation of data sets with synthetic ground truth

To cover a wide range of frequencies and avoid tedious manual ground truth checking, we design two synthetic data sets of seismic traces from the sum of two sinusoids with varying frequency gradients. Moreover, their corresponding synthetic ground truth instantaneous frequencies are derived and generated. The challenge here is to come up with an analytical formula for the automatic calculation of the instantaneous frequency from two composited sinusoids.

Following Cohen (1995), we represent the two sinusoids as complex analytic functions $z_1(t)$ and $z_2(t)$:

$$z_1(t) = a_1 \cos(\omega_1 t) + i a_1 \sin(\omega_1 t) \tag{7}$$

and

$$z_2(t) = a_2 \cos(\omega_2 t) + i a_2 \sin(\omega_2 t), \tag{8}$$

where a_1 and a_2 are the amplitudes and ω_1 and ω_2 are the angular frequencies, which equal to $2\pi f_1$ and $2\pi f_2$, respectively. Their sum is the complex trace $z(t)$:

$$\begin{aligned} z(t) &= z_1(t) + z_2(t) \\ &= a_1 \cos(\omega_1 t) + a_2 \cos(\omega_2 t) \\ &\quad + i(a_1 \sin(\omega_1 t) + a_2 \sin(\omega_2 t)). \end{aligned} \tag{9}$$

The real part of $z(t)$ is regarded as the composited seismic trace, and the imaginary part is the corresponding Hilbert-transformed trace. The behavior of $z(t)$ can be described by a phasor diagram as shown in Figure 2. The instantaneous amplitude $a(t)$ of the complex trace $z(t)$ is

$$a(t) = \sqrt{a_1^2 + a_2^2 + 2a_1 a_2 \cos(\omega_2 - \omega_1)t}. \tag{10}$$

The corresponding instantaneous phase and instantaneous frequency $\theta(t)$ and $f(t)$ are

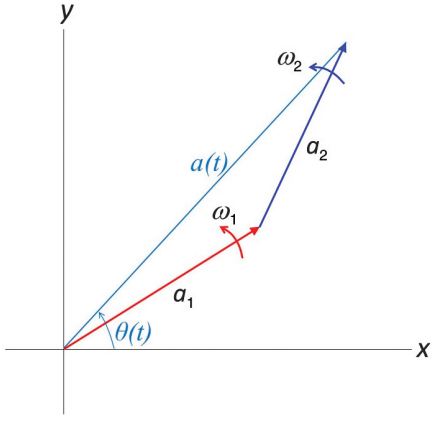

Figure 2. Phasor diagram with instantaneous amplitude $a(t)$ and instantaneous phase $\theta(t)$ for the sum of two sinusoids with amplitudes a_1 and a_2 and angular frequencies ω_1 and ω_2.

$$\theta(t) = \tan^{-1}\left(\frac{a_1 \sin(\omega_1 t) + a_2 \sin(\omega_2 t)}{a_1 \cos(\omega_1 t) + a_2 \cos(\omega_2 t)}\right) \tag{11}$$

$$f(t) = \frac{1}{2\pi}\frac{a_1^2\omega_1 + a_2^2\omega_2 + a_1 a_2(\omega_1 + \omega_2)\cos((\omega_1 - \omega_2)t)}{a_1^2 + a_2^2 + 2a_1 a_2 \cos(\omega_1 - \omega_2)t}. \tag{12}$$

Equations 10–12 can also be derived either from the definitions by the authors or equations 2.80 and 2.81 in Cohen's (1995) book. The detailed derivations are provided in Appendices A and B, respectively. To better understand those equations, seismic traces and synthetic ground truth instantaneous frequencies are graphed on single trace under different amplitudes and angular frequencies in Figure 3a. Specifically, the red line has an instantaneous frequency between 20 and 55 Hz, which is the prime seismic data range. The instantaneous frequency of the green line is below 43 Hz, and that of the blue line is above 64 Hz. Moreover, in Figure 3b, the four reviewed classic algorithms are compared on the prime seismic data range, where all the algorithms should be tuned for.

To compare various instantaneous frequency algorithms comprehensively, instead of with a single trace, synthetic data sets with seismic traces and synthetic ground truth instantaneous frequencies are generated on 3D cubes, respectively, a wide range of angular frequencies are fed to ω_1 in equation 7, and ω_2 in equation 8, respectively, together with sets of constant radii/amplitudes a_1 and a_2, which result in different frequency ranges. In particular, ω_1 and ω_2 vary along the inline and crossline axes linearly, in the range of $[0, 250\pi]$ with a step of 2π. The sample number is 501 with sample rate of 4 ms. Thus, the synthetic data set is $126 \times 126 \times 501$ in order of inline, crossline, and time. Moreover, a_1 and a_2 are fixed to 1 and 0.5 for data set 1, and 1 and 1.05 for data set 2, respectively. Thereby, based on the real part of $z(t)$ in equation 9, data set 1 has seismic trace amplitude in $[-1.5, 1.5]$, whereas data set 2 in $[-2.05, 2.05]$. Based on equation 12, data set 1 has synthetic ground truth instantaneous frequency in $[-125, 250]$, whereas data set 2 in $[-2500, 2625]$. Specifically, data set 2 has large spike and negative frequencies, thus testing a different scenario. Specific slices from the two seismic trace data sets (the real part of $z(t)$ in equation 9) are shown in Figure 4a1 and 4a2 and their synthetic ground truth instantaneous frequency (equation 12) in Figure 4b1 and 4b2. These slices are randomly selected, among those that cover the different regions that we define later. Both synthetic seismic trace data sets are available for downloading from A3Mark to test instantaneous frequency algorithms. Although their "ground truth" is not downloadable, it is used for calculating the quality metrics implicitly when you upload your algorithm's result.

There is a potential singularity in equation 12, which appears when $a_1 = a_2$. Fortunately, we can prove that in that singularity case, the instantaneous frequency reduces to $(\omega_1 + \omega_2)/4\pi$.

The definition for instantaneous frequency does include a phase difference term, but we observe that in the extreme case, in which the cosine of the phase difference is zero (i.e., the two frequencies are at orthogonal phase), the instantaneous frequency is the energy-weighted average of the two input frequencies, that is $(a_1^2\omega_1 + a_2^2\omega_2)/2\pi(a_1^2 + a_2^2)$.

In addition, if $(\omega_1 - \omega_2)t = \pm 180°$, $a_1 = 1$, $a_2 = 1 + \delta$, then $f(t) = (\omega_2 + (\omega_2 - \omega_1)/\delta)/2\pi$. Now, if $\omega_1 \neq \omega_2$, then we may

have negative frequency and infinitely large frequencies, as δ approaches zero. Thus, there are no upper or lower bounds on the theoretically possible instantaneous frequency, implying that it is not bound by the Nyquist frequency.

Region-based quality metrics

To evaluate the performance of numerous instantaneous frequency algorithms, we need a quantitative way to measure the difference between their output and the synthetic ground truth. The ground truth is also given as labeled regions, that is, sets of labeled points to reflect the aforementioned algorithmic issues, which are defined as follows:

- Negative: $(-\infty, 0\ \text{Hz})$.
- Edge: [0 ms, len] & [2000 ms-len, 2000 ms] in time axis for filter tail issue, and $\text{len} = \min(100\ \text{ms}, 1000\ \text{ms}/\min(\omega_1/2\pi, \omega_2/2\pi))$.
- Low: [0 Hz, 6 Hz) & (−6 Hz, 0 Hz].
- Half-Nyquist: [6 Hz, 62.5 Hz) & (−62.5 Hz, −6 Hz].
- Nyquist: [62.5 Hz, 125 Hz) & (−125 Hz, −62.5 Hz].
- Spike: [125 Hz, ∞) & (−∞, −125 Hz].
- Full: (−∞, ∞).

Those regions are labeled as {−1, 0, 1, 2, 3, 4} for {negative, edge, low, half-Nyquist, Nyquist, spike} and are visualized by the respective rainbow color bands {red, orange, yellow, green, blue, purple} in Figure 4c1 and 4c2. The selected inline, crossline, and time slice are intended to be representative of instantaneous frequency regions and give a comprehensive illustration. For each region, the mean absolute error (MAE) and root-mean square (rms) error can be used as difference metrics between an algorithm's output and the synthetic ground truth. However, the instantaneous frequency can assume very large values, beyond the Nyquist, and large spikes in the difference plots can thus be expected. These spikes will considerably impact the MAE and rms error scores and may thus not give representative values for the "average" performance. We, therefore, first detect and classify these large spikes as outliers using

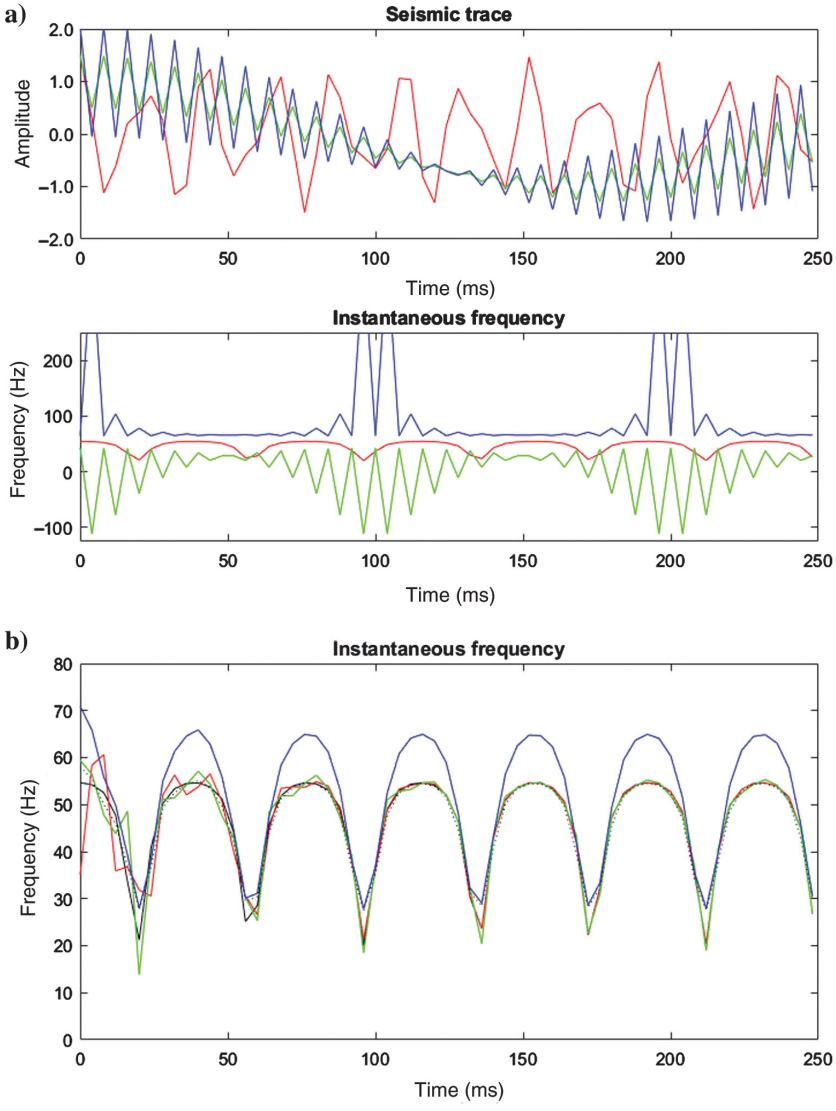

Figure 3. (a) Composite seismic trace and synthetic ground truth instantaneous frequency on a single trace from two sinusoids with different amplitudes and angular frequencies — red line: $a_1 = 1$, $a_2 = 0.5$, $\omega_1 = 92\pi$, $\omega_2 = 144\pi$; green line: $a_1 = 1$, $a_2 = 0.5$, $\omega_1 = 6\pi$, $\omega_2 = 246\pi$; and blue line: $a_1 = 1$, $a_2 = 1.05$, $\omega_1 = 6\pi$, $\omega_2 = 246\pi$. (b) Comparison of four classic algorithms' output on the prime seismic data range — solid black line, synthetic ground truth instantaneous frequency; solid red line, exact formula by Taner et al.; solid green line, frequency domain approach by Hardage; solid blue line, Claerbout approximation; and dotted black line, Scheuer and Oldenburg approximation.

a custom threshold value, which is 80% of the mean value of the synthetic ground truth in that region. Thus, one metric is the percentage of the outliers (outliers_PCT). When these outliers are excluded, MAE and rms error are calculated on the inliers, giving the inliers_MAE and inliers_rms error metrics. Specifically, outliers_PCT is in the range [0, 1], and inlier metrics are in the range [0, inf) — the smaller the better. In addition to the original synthetic ground truth of instantaneous frequency (IF), the vertical change in instantaneous frequency (dIF) is computed on all seven regions as well.

RESULTS AND DISCUSSION

In addition to the four noncommercial classic instantaneous frequency algorithms reviewed in the section of instantaneous frequency, we also test the instantaneous frequency on four commercial software packages with generic names, such as "product A," "product B," "product C," and "product D," to avoid commercialism issues. Tables 1 and 2 summarize the quality metrics of all the eight instantaneous frequency algorithms on the two synthetic data sets, and Figures 5 and 6 are the difference/error images between the algorithm output and the synthetic ground truth of the instantaneous frequency. All of the numerical and visual results have also been uploaded on the free academic seismic attribute benchmarking service A3Mark, which allows users to submit the results on their own algorithms or any software that they have access to.

As can be observed in the tables, the "best" algorithm for the instantaneous frequency in most circumstances is the frequency-domain algorithm described by Hardage (1987), in which the Hilbert transform and the trace derivatives are computed in the frequency domain. It is also by far the fastest approach. The performance of the exact time-domain formula given by Taner et al. (1979) is closest to the frequency-domain algorithm but much slower because of the need for long convolutional operators for the Hilbert transform operator and the derivative operators, as stated above. The illustrations of Figures 5 and 6 confirm the numerical results from the metrics, where Figures 5a, 5b, 6a, and 6b are close to zero in most regions. The reason behind this is that both methods use formulas that closely approximate the definition of instantaneous frequency. The difference between them should be primarily in their filter tails, or at points of abrupt change, which are often at the beginning and ending of the data. This can be seen in Figures 5 and 6, where Figures 5a and 6a have more red at inline 3, crossline 123/125, especially at the left edge side of crossline 123/125 and time slice −1004/−1008, but not inline 100 and the rest of time slices −1004/−1008, when compared with Figures 5b and 6b. The only reason for not using the frequency-domain algorithm routinely is

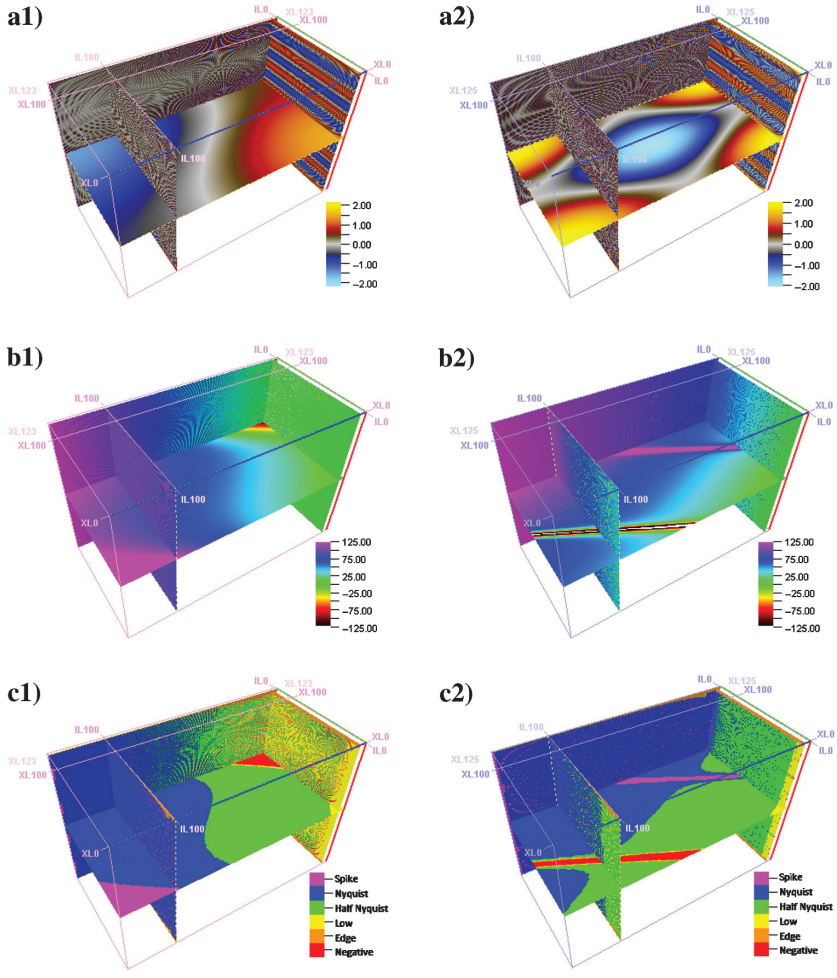

Figure 4. Illustrations of the synthetized seismic test data sets and their synthetic ground truths of instantaneous frequency, as well as the labeled instantaneous frequency regions. DATA SET 1 at inlines 3 and 100, crossline 123, time −1004: (a1) seismic trace, (b1) synthetic ground truth of the instantaneous frequency, (c1) instantaneous frequency regions {negative, edge, low, half-Nyquist, Nyquist, spike}, DATA SET 2 at inlines 3 and 100, crossline 125, time −1008: (a2) seismic trace, (b2) synthetic ground truth of the instantaneous frequency, (c2) instantaneous frequency regions {negative, edge, low, half-Nyquist, Nyquist, spike}. The aliasing effect is present in the data set itself and is not due to the display method.

Table 1. Instantaneous frequency (IF) results on synthetic data set 1. Green/small is better than red/large.

Region	Metrics	Non-Commercial								Commercial							
		Exact formula by Taner et al.		Frequency domain approach by Hardage		Claerbout approximation		Scheuer and Oldenburg approximation		Instantaneous frequency of Product A		Instantaneous frequency of Product B		Instantaneous frequency of Product C		Instantaneous frequency of Product D	
		IF	dIF	IF	dIF	IF	dIF	IF	dIF	IF	dIF	IF	dIF	IF	dIF	IF	dIF
Low	Outliers_PCT	0.19	0.16	0.09	0.33	0.55	0.17	0.55	0.17	0.66	0.24	0.68	0.24	0.71	0.19	0.68	0.18
	Inliers_MAE	0.38	0.14	0.59	0.57	0.82	0.20	0.83	0.20	0.74	0.17	0.52	0.15	0.66	0.18	0.40	0.12
	Inliers_rms error	0.64	0.26	0.76	0.65	1.07	0.33	1.07	0.33	0.98	0.29	0.86	0.30	0.92	0.32	0.73	0.29
Half Nyquist	Outliers_PCT	0.02	0.05	0.00	0.02	0.05	0.21	0.05	0.20	0.09	0.23	0.11	0.33	0.09	0.28	0.09	0.28
	Inliers_MAE	1.22	0.62	0.72	0.95	7.25	2.28	4.93	1.94	4.59	1.84	5.20	2.29	7.08	1.97	7.09	1.94
	Inliers_RMSE	3.82	1.77	1.95	1.64	9.78	3.77	8.45	3.47	8.05	3.33	8.64	3.72	10.10	3.42	10.14	3.40
Nyquist	Outliers_PCT	0.02	0.09	0.01	0.04	0.39	0.59	0.14	0.26	0.04	0.22	0.08	0.37	1.00	1.00	1.00	1.00
	Inliers_MAE	3.44	0.43	0.94	0.63	31.62	1.51	3.73	0.85	4.82	0.93	6.19	1.32	N/A	N/A	N/A	N/A
	Inliers_rms error	10.50	1.00	3.70	1.06	36.37	2.17	7.85	1.54	8.98	1.65	11.41	1.94	N/A	N/A	N/A	N/A
Spike	Outliers_PCT	0.12	0.52	0.05	0.17	0.79	0.88	1.00	1.00	1.00	1.00	1.00	1.00	1.00	1.00	1.00	1.00
	Inliers_MAE	11.54	1.42	1.51	1.30	69.60	2.30	N/A	N/A	N/A	N/A	N/A	N/A	N/A	N/A	N/A	N/A
	Inliers_rms error	27.57	2.52	3.68	2.08	77.33	3.54	N/A	N/A	N/A	N/A	N/A	N/A	N/A	N/A	N/A	N/A
Negative	Outliers_PCT	0.13	0.25	0.02	0.05	0.53	0.35	0.54	0.35	1.00	1.00	0.60	0.60	0.81	0.41	0.80	0.40
	Inliers_MAE	2.20	1.23	1.38	1.55	9.02	2.69	9.05	2.71	N/A	N/A	10.38	2.55	12.71	2.82	12.36	2.72
	Inliers_rms error	4.92	2.31	2.79	2.10	11.20	3.62	11.25	3.65	N/A	N/A	12.30	3.50	14.29	3.76	14.00	3.71
Edge	Outliers_PCT	0.06	0.36	0.01	0.13	0.22	0.42	0.12	0.30	0.20	0.45	0.17	0.50	0.24	0.36	0.24	0.36
	Inliers_MAE	10.49	7.68	6.65	6.85	11.72	5.44	7.80	5.05	10.85	5.62	11.45	5.87	12.50	4.05	12.49	4.04
	Inliers_rms error	14.37	9.23	9.39	8.45	15.84	7.36	11.54	6.77	15.59	7.66	16.22	7.96	17.62	6.51	17.61	6.51
Full	Outliers_PCT	0.03	0.07	0.01	0.02	0.27	0.38	0.11	0.27	0.09	0.25	0.09	0.37	0.26	0.34	0.26	0.34
	Inliers_MAE	2.43	0.92	0.93	1.00	15.28	3.48	5.07	2.48	5.68	2.59	7.07	3.11	18.03	3.29	18.04	3.27
	Inliers_rms error	8.16	2.49	3.97	1.95	21.96	5.37	9.42	4.37	10.52	4.51	12.64	4.93	25.27	5.17	25.32	5.16

Table 2. Instantaneous frequency (IF) results on synthetic data set 2. Green/small is better than red/large.

Region	Metrics	Non-Commercial								Commercial							
		Exact formula by Taner et al.		Frequency domain approach by Hardage		Claerbout approximation		Scheuer and Oldenburg approximation		Instantaneous frequency of Product A		Instantaneous frequency of Product B		Instantaneous frequency of Product C		Instantaneous frequency of Product D	
		IF	dIF	IF	dIF	IF	dIF	IF	dIF	IF	dIF	IF	dIF	IF	dIF	IF	dIF
Low	Outliers_PCT	0.24	0.27	0.26	0.87	0.43	0.20	0.46	0.20	0.48	0.66	0.43	0.10	0.76	0.57	0.42	0.07
	Inliers_MAE	0.63	0.07	0.77	0.12	0.70	0.07	0.65	0.07	0.62	0.74	0.13	0.01	1.35	0.04	0.15	0.02
	Inliers_rms error	0.91	0.10	1.05	0.13	0.99	0.10	0.93	0.10	0.89	0.98	0.40	0.03	1.57	0.07	0.39	0.03
Half Nyquist	Outliers_PCT	0.02	0.11	0.00	0.08	0.24	0.49	0.27	0.40	0.29	0.09	0.17	0.37	0.53	0.47	0.08	0.21
	Inliers_MAE	1.35	0.29	1.04	0.74	6.76	0.74	2.71	0.45	2.45	4.59	1.93	0.56	17.85	1.17	7.84	0.52
	Inliers_rms error	4.20	0.66	2.77	1.02	10.07	1.21	6.91	0.90	6.52	8.05	4.86	0.97	20.03	1.61	11.35	0.98
Nyquist	Outliers_PCT	0.02	0.17	0.01	0.09	0.34	0.75	0.15	0.39	0.10	0.04	0.16	0.39	1.00	1.00	1.00	1.00
	Inliers_MAE	5.73	0.39	2.53	0.64	31.93	0.94	11.42	0.43	13.07	4.82	3.01	0.70	N/A	N/A	N/A	N/A
	Inliers_rms error	15.24	0.75	9.99	0.95	36.92	1.37	24.26	0.86	25.51	8.98	8.41	1.07	N/A	N/A	N/A	N/A
Spike	Outliers_PCT	0.11	0.46	0.05	0.21	0.39	0.59	1.00	1.00	1.00	1.00	1.00	1.00	1.00	1.00	1.00	1.00
	Inliers_MAE	35.90	3.84	32.18	5.52	201.01	4.87	N/A	N/A	N/A	N/A	N/A	N/A	N/A	N/A	N/A	N/A
	Inliers_rms error	78.55	7.12	66.29	7.51	211.76	9.04	N/A	N/A	N/A	N/A	N/A	N/A	N/A	N/A	N/A	N/A
Negative	Outliers_PCT	0.11	0.24	0.05	0.12	0.34	0.39	0.34	0.39	1.00	1.00	0.35	0.72	1.00	1.00	0.37	0.39
	Inliers_MAE	21.15	4.04	21.21	7.41	72.55	7.72	73.27	7.50	N/A	N/A	80.97	10.22	N/A	N/A	94.00	8.07
	Inliers_rms error	47.20	7.48	41.53	9.90	94.57	11.50	95.14	11.19	N/A	N/A	99.00	12.99	N/A	N/A	109.59	11.95
Edge	Outliers_PCT	0.09	0.22	0.06	0.14	0.30	0.41	0.29	0.37	0.35	0.20	0.25	0.48	0.39	0.14	0.16	0.13
	Inliers_MAE	12.43	13.12	7.56	8.28	14.71	9.00	7.88	5.61	13.28	10.85	8.85	6.65	27.67	5.64	15.82	3.60
	Inliers_rms error	17.40	15.92	11.30	11.09	21.07	12.70	14.56	8.72	20.93	15.59	14.18	10.61	31.28	8.83	22.36	7.39
Full	Outliers_PCT	0.03	0.06	0.02	0.03	0.27	0.40	0.18	0.33	0.16	0.09	0.18	0.37	0.44	0.14	0.17	0.13
	Inliers_MAE	4.42	2.07	1.56	1.97	25.77	7.11	10.18	3.49	11.60	5.68	2.58	2.51	48.58	5.34	31.03	3.25
	Inliers_rms error	15.38	5.44	8.15	4.49	37.12	11.38	23.77	7.74	26.16	10.52	8.12	5.77	58.76	8.56	44.53	6.91

that, when it fails, it fails catastrophically like many frequency-domain methods. This is because its filter tails are effectively as long as the input data.

The approximations given by Claerbout (1985) and Scheuer and Oldenburg (1988) perform differently, especially in high-frequency regions (corresponding to the orange region in Figure 4c1 and 4c2), as shown in the left part of the cubes in Figure 5c and 5d and the left and top parts of the cubes in Figure 6c and 6d, where Figures 5d and 6d are better than Figures 5c and 6c. As can be deduced from the tables, these two approximations are almost equal in low, half-Nyquist, and negative regions. However, Scheuer and Oldenburg's approximation is better than Claerbout's approximations in the Nyquist and edge regions but not the spike region, in which the spike magnitude is limited to the Nyquist frequency. Overall, the approximation of Scheuer and Oldenburg is robust and better than that of Claerbout. Both methods, like all the others, depend on the Hilbert transform, which, if not well-designed, can introduce errors independently of which formula one uses.

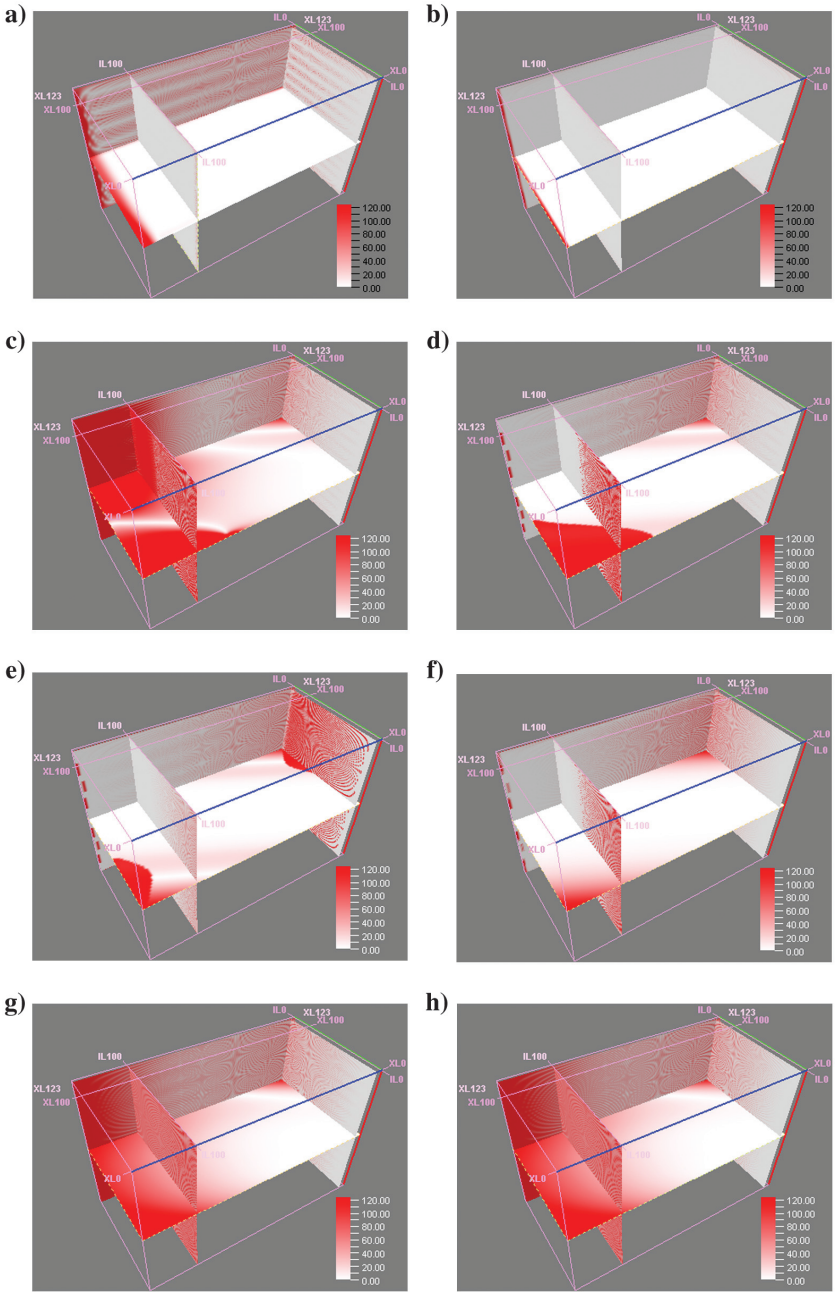

Figure 5. Illustrations of the difference (error) of eight instantaneous frequency computations: (a) exact formula by Taner et al., (b) frequency domain approach by Hardage, (c) Claerbout approximation, (d) Scheuer and Oldenburg approximation, and (e-h) instantaneous frequency of product A-D on seismic data set 1 at inlines 3 and 100, crossline 123, time −1004.

Different from the mathematical approximations and products C and D, products A and B have relatively good performance in high frequencies, such as the orange Nyquist region in Figure 4c1 and 4c2, although both spikes are within the Nyquist frequency, as shown in the tables. It can be seen from Figures 5 and 6, that Figures 5e, 5f, 6e, and 6f have less red than Figures 5g, 5h, 6g, and 6h and are comparable with Figures 5d and 6d, in their left and top parts. Moreover, product A has no negative frequencies, and product B performs better than products C and D in the negative frequency region. A small difference can be noticed in the region of Figure 5e and 5f and Figure 6e and 6f that corresponds to the purple region of Figure 4c1 and 4c2; also Figures 5f and 6f seem slightly better than Figures 5e and 6e. Products A and B perform similarly in the low-frequency region when compared with product D, but they are slightly better than product C, as can be seen from the tables. In particular, as clearly visible in Figure 5, but not Figure 6, product B (Figure 5f) has much less red than product A (Figure 5e) in inline 3 (corresponding to the green region in Figure 4c1 and 4c2).

The performance of instantaneous frequency in product D is superior to product C. As shown in the tables, product D outperforms product C only in the low-frequency region in Table 1 and all regions in Table 2. This can be confirmed from Figures 5g, 5h, 6g, and 6h, where Figure 5g and 5h does not have a clearly noticeable difference, whereas Figure 6h has much less red than Figure 6g. This improvement is because the maximum operator length for the Hilbert transform is much longer in the newer package, with a maximum length of 1.0 s, thus leading to more accurate results for low-frequency data (down to approximately 3 Hz), as stated above. However, low-frequency results (corresponding to the green regions in Figure 4c1 and 4c2 and Figures 5g, 5h, 6g, and 6h) do not exhibit this difference because of the limited contrast in the low-frequency region of the color bar; the difference is shown visually with the "seismic default" color bar in Xing et al. (2017). Moreover, products C and D have poor quality in the high-frequency region (corresponding to the orange and red regions in Figure 4c1 and 4c2), as shown on the left side of the cube in Figure 5g

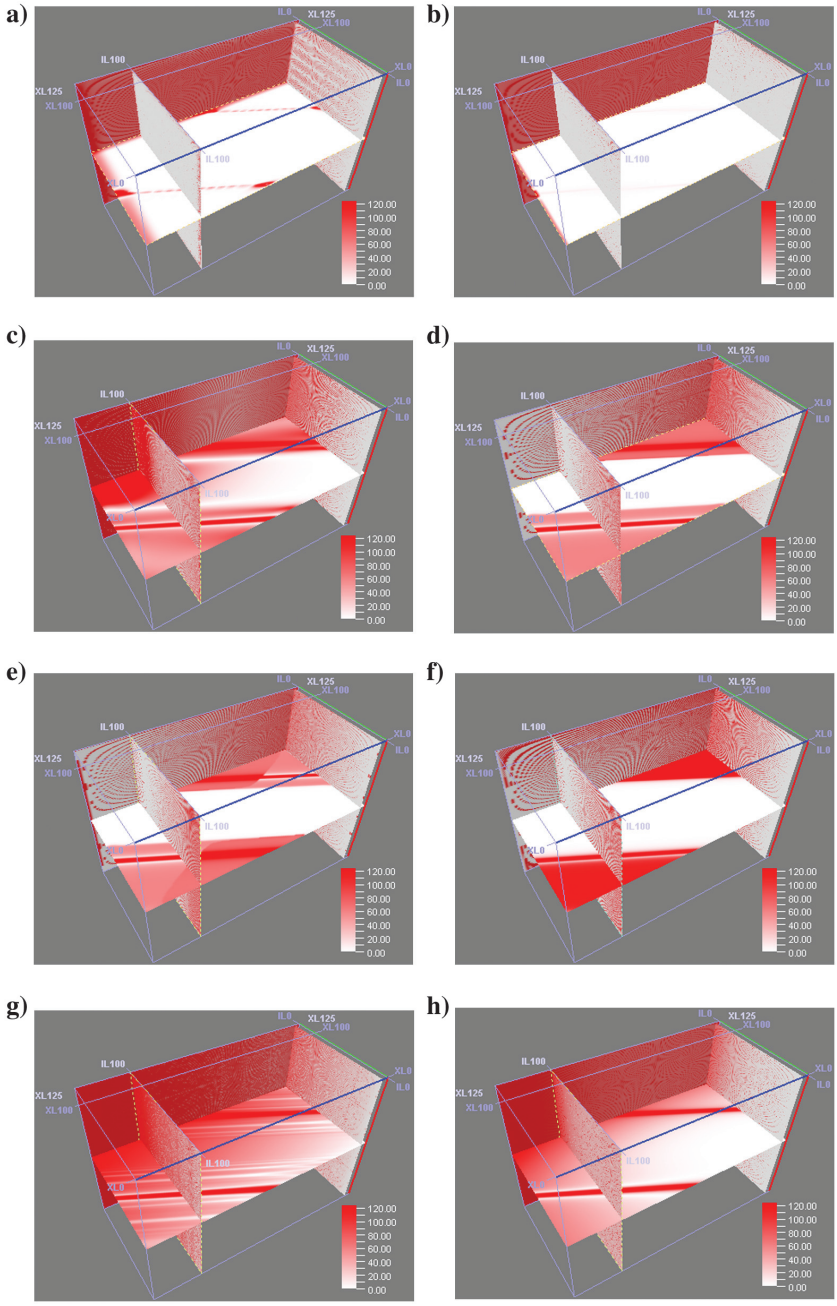

Figure 6. Illustrations of the difference (error) of eight instantaneous frequency computations: (a) exact formula by Taner et al., (b) frequency domain approach by Hardage, (c) Claerbout approximation, (d) Scheuer and Oldenburg approximation, and (e-h) instantaneous frequency of Product A-D on seismic data set 2 at inlines 3 and 100, crossline 125, time −1008.

and the left and top sides of the cube in Figure 6h. This is due to the aliasing issue for frequencies above half-Nyquist, which occurs due to a poor choice of differentiation operator, similar to the problem with Claerbout's approximation.

CONCLUSION

Numerous instantaneous frequency computations exist in noncommercial algorithms and commercial E&P software tools, and they all have different implementation issues. We propose a robust and reliable scientific process to objectively compare different implementations of instantaneous frequency. In particular, two synthetic seismic test data sets, which are based on the sum of two oscillating functions with varying frequencies and constant amplitudes, are generated. Correspondingly, their instantaneous frequency synthetic ground truths are calculated analytically. Most importantly, we derive the theoretical foundation of the ground truth instantaneous frequencies step by step from two composited sinusoids and illustrate it with a simple analytical model. In addition, we design several region-based quality metrics to investigate the issues pointed out for various instantaneous frequency algorithms. The experiments reported here demonstrate the performance in different regions of various instantaneous frequency algorithms, quantitatively and qualitatively. In general, the frequency domain approach by Hardage is the best.

A3Mark, the free academic online benchmarking service for seismic attributes, has been extended to include instantaneous frequency benchmarking. Users and developers of commercial or open source instantaneous frequency algorithms can upload their results to A3Mark at any time.

ACKNOWLEDGMENTS

Many thanks to J. Xu (maverick.xu@hotmail.com) for helping out with the web service and reviewers for their valuable comments. This research was supported in part by NTNU and Schlumberger AS.

DATA AND MATERIALS AVAILABILITY

Data associated with this research are available and can be accessed via the following URL: http://a3mark.idi.ntnu.no/.

APPENDIX A

INSTANTANEOUS FREQUENCY DERIVATION FOR THE SUM OF TWO SINUSOIDS, STARTING FROM ORIGINAL DEFINITIONS

For the sum of two sinusoids, represented as a complex trace in equation 9, let $A(t)$ be the real part and $B(t)$ be the imaginary part. Then

$$A(t) = a_1 \cos(\omega_1 t) + a_2 \cos(\omega_2 t) \qquad \text{(A-1)}$$

and

$$B(t) = a_1 \sin(\omega_1 t) + a_2 \sin(\omega_2 t). \qquad \text{(A-2)}$$

These have time derivatives $A'(t)$ and $B'(t)$, given by

$$A' = -[a_1\omega_1 \sin(\omega_1 t) + a_2\omega_2 \sin(\omega_2 t)] \tag{A-3}$$

and

$$B' = a_1\omega_1 \cos(\omega_1 t) + a_2\omega_2 \cos(\omega_2 t). \tag{A-4}$$

Recalling the definition of the angular frequency, the practical equation for its computation is derived as follows, as given in Taner et al. (1979)

$$\omega(t) = \frac{B'A - BA'}{A^2 + B^2}. \tag{A-5}$$

The numerator of equation A-5 becomes

$$\begin{aligned} &B'A - BA' \\ &= a_1^2\omega_1 + a_2^2\omega_2 + a_1a_2(\omega_1 + \omega_2)[\sin(\omega_1 t)\sin(\omega_2 t) \\ &+ \cos(\omega_1 t)\cos(\omega_2 t)] \\ &= a_1^2\omega_1 + a_2^2\omega_2 + a_1a_2(\omega_1 + \omega_2)\cos((\omega_1 - \omega_2)t) \end{aligned} \tag{A-6}$$

and the denominator becomes

$$\begin{aligned} &A^2 + B^2 \\ &= a_1^2 + a_2^2 + 2a_1a_2[\sin(\omega_1 t)\sin(\omega_2 t) + \cos(\omega_1 t)\cos(\omega_2 t)] \\ &= a_1^2 + a_2^2 + 2a_1a_2\cos((\omega_1 - \omega_2)t). \end{aligned} \tag{A-7}$$

Putting the numerator and denominator together, the equation for the angular frequency $\omega(t)$ of the sum of two sinusoids is

$$\omega(t) = \frac{a_1^2\omega_1 + a_2^2\omega_2 + a_1a_2(\omega_1 + \omega_2)\cos((\omega_1 - \omega_2)t)}{a_1^2 + a_2^2 + 2a_1a_2\cos((\omega_1 - \omega_2)t)}. \tag{A-8}$$

Finally, to convert to instantaneous frequency $f(t)$ with units of hertz,

$$f(t) = \omega(t)/2\pi. \tag{A-9}$$

APPENDIX B

INSTANTANEOUS FREQUENCY DERIVATION FOR THE SUM OF TWO SINUSOIDS, STARTING FROM EQUATIONS BY COHEN (1995)

For the two oscillating seismic traces of equation 9, just as in Appendix A, Cohen (1995, p. 40) has derived equations for instantaneous amplitude $a(t)$ and for instantaneous angular frequency $\omega(t)$ as follows:

$$a^2(t) = a_1^2 + a_2^2 + 2a_1a_2\cos(\omega_2 - \omega_1)t, \tag{B-1}$$

$$\begin{aligned} \omega(t) = \varphi'(t) &= \left(\arctan\frac{a_1 \sin\omega_1 t + a_2 \sin\omega_2 t}{a_1\cos\omega_1 t + a_2\cos\omega_2 t}\right)' \\ &= \frac{\omega_2 + \omega_1}{2} + \frac{\omega_2 - \omega_1}{2}\frac{a_2^2 - a_1^2}{a^2(t)}. \end{aligned} \tag{B-2}$$

Starting from these equations, we insert $a(t)$ into $\omega(t)$ to obtain

$$\begin{aligned} \omega(t) &= \frac{\omega_1 a^2 + \omega_2 a^2 + (\omega_2 - \omega_1)(a_2^2 - a_1^2)}{2a^2} \\ &= \frac{\omega_1(a_1^2 + a_2^2 + 2a_1a_2\cos(\omega_2 - \omega_1)t)}{2a^2} \\ &+ \frac{\omega_2(a_1^2 + a_2^2 + 2a_1a_2\cos(\omega_2 - \omega_1)t)}{2a^2} \\ &+ \frac{(\omega_2 - \omega_1)(a_2^2 - a_1^2)}{2a^2} \\ &= \frac{\omega_1 a_1^2 + \omega_2 a_2^2 + (\omega_1 + \omega_2)a_1a_2\cos(\omega_2 - \omega_1)t}{a^2} \\ &= \frac{\omega_1 a_1^2 + \omega_2 a_2^2 + (\omega_1 + \omega_2)a_1a_2\cos(\omega_2 - \omega_1)t}{a_1^2 + a_2^2 + 2a_1a_2\cos(\omega_2 - \omega_1)t}, \end{aligned} \tag{B-3}$$

which is equivalent to the authors' derivation in Appendix A.

REFERENCES

Barnes, A. E., 2006, Too many seismic attributes?: CSEG Recorder, **31**, 41–45.

Battista, B. M., C. Knapp, T. McGee, and V. Goebel, 2007, Application of the empirical mode decomposition and Hilbert-Huang transform to seismic reflection data: Geophysics, **72**, no. 2, H29–H37, doi: 10.1190/1.2437700.

Chopra, S., and K. J. Marfurt, 2005, Seismic attributes — A historical perspective: Geophysics, **70**, no. 5, 3SO–28SO, doi: 10.1190/1.2098670.

Claerbout, J. F., 1985, Fundamentals of geophysical data processing: Blackwell Scientific Publications.

Cohen, L., 1995, Time-frequency analysis: Prentice-Hall PTR.

Hardage, B. A., 1987, Seismic stratigraphy: Handbook of geophysical exploration: Geophysical Press, Section I, Seismic exploration 9.

Hardy, H. H., R. A. Beier, and J. D. Gaston, 2003, Frequency estimates of seismic traces: Geophysics, **68**, 370–380, doi: 10.1190/1.1543222.

Lu, W., and C. K. Zhang, 2011, A robust instantaneous frequency estimation method: 73rd Annual International Conference and Exhibition, EAGE, Extended Abstracts, P093, doi: 10.3997/2214-4609.20149432.

PetroWiki, 2019, Seismic attributes, http://petrowiki.org/index.php?title=Seismic_attributes&printable=yes, accessed 16 January 2019.

Scheuer, T. E., and D. W. Oldenburg, 1988, Local phase velocity from complex seismic data: Geophysics, **53**, 1503–1511, doi: 10.1190/1.1442431.

SEG wiki, 2019, Seismic attribute, http://wiki.seg.org/wiki/Dictionary:Attribute,_seismic, accessed 16 January 2019.

Taner, M. T., F. Koehler, and R. E. Sheriff, 1979, Complex seismic trace analysis: Geophysics, **44**, 1041–1063, doi: 10.1190/1.1440994.

Taner, M. T., J. S. Schuelke, R. O'Doherty, and E. Baysal, 1994, Seismic attributes revisited: 64th Annual International Meeting, SEG, Expanded Abstracts, 1104–1106, doi: 10.1190/1.1822709.

Taner, M. T., and R. E. Sheriff, 1977, Application of amplitude, frequency, and other attributes to stratigraphic and hydrocarbon determination: AAPG Memoir, **26**, 301–327.

Ville, J., 1948, Théories et applications de la notion de signal analytique: Cables et Transmission, **2**, 61–74.

Wang, P., and J. H. Gao, 2012, The extraction of instantaneous frequency from seismic data based on the GMWs: 82nd Annual International Meeting, SEG, Expanded Abstracts, doi: 10.1190/segam2012-0902.1.

Xing, L., V. Aarre, A. Barnes, T. Theoharis, N. Salman, and E. Tjåland, 2017, Instantaneous frequency seismic attribute benchmarking: 87th Annual International Meeting, SEG, Expanded Abstracts, 2086–2090, doi: 10.1190/segam2017-17672950.1.

Xing, L., V. Aarre, N. Salman, T. Theoharis, and E. Tjåland, 2018, A3Mark: Seismic attribute benchmarking: Geophysics, **83**, no. 1, O15–O24, doi: 10.1190/geo2017-0013.1.

Yilmaz, Ö., 2001, Seismic data analysis: Processing, inversion, and interpretation of seismic data: SEG Investigations in Geophysics 10.